# A Finite-Element Method for the Plastic Buckling Analysis of Plates

ALLAN PIFKO* AND GABRIEL ISAKSON†
*Grumman Aerospace Corporation, Bethpage, N. Y.*

**An existing finite-element technique for elastic buckling of plates is extended to include the case of plastic buckling. The Stowell theory for the plastic buckling of flat plates is used in conjunction with the finite-element technique. Application is made to rectangular plates and results are presented for a variety of boundary support conditions and several different edge loading conditions.**

## Introduction

IN the present paper, a finite-element technique previously presented in Refs. 1–3 for elastic buckling of plates is extended to include the case of plastic buckling. In order to predict buckling, the decrease in stiffness which results from the action of compressive membrane stress must be taken into account. The finite-element buckling analysis accomplishes this by introducing an additional component part to the usual elastic bending stiffness matrix. This additional component part is derived from energy considerations when terms representing the work done by in-plane deformations are included in the expression for the strain energy functional. When this state of stress is compressive, the inclusion of this matrix has the effect of reducing the stiffness of the structure, as characterized by the stiffness matrix. A discussion of the significance and consistent development of this matrix can be found in Ref. 4. In accordance with the terminology of that work, we refer to the additional matrix as the initial stress stiffness matrix.

In the present paper, the approach taken for the plastic buckling analysis of plates conceptually follows the aforementioned approach. That is, the stiffness matrix is further modified to include the effect of the altered stiffness properties of the material associated with plastic deformation prior to buckling. This modification is effected by altering the usual elastic bending stiffness matrix so that it contains coefficients which depend on the state of plasticity in the structure and, therefore, the state of stress.

The extent to which the elastic bending stiffness matrix is modified depends on the plastic buckling theory used. At present, the status of the plastic buckling problem is somewhat confused. Although the plastic buckling phenomenon is well understood in the case of columns, the same cannot be said of plates and shells. The essential difference is that in the former the stresses are uniaxial, whereas in the latter they are biaxial and may assume a substantially different distribution among components during buckling than exists prior to buckling. This makes an analytical solution quite sensitive to the type of plasticity theory that is used.

Plastic buckling analyses based both on flow theory and on deformation theory have been used, the former, for instance, in Refs. 5 and 6 and the latter in Refs. 7–9. A comparison of results from some of these references with experimental data[10] shows the deformation theory results to be in better agreement with experiment than those of the flow theory. This is paradoxical since, in the case of some simple stable structures, flow theory provides results that are in better agreement with experiment than corresponding results using deformation theory. Furthermore, deformation theory contains fundamental inconsistencies not present in flow theory.

Two different explanations have been offered for the inaccuracy of flow theory in this problem. One of these is that the Lévy-Mises flow theory, based on the second invariant of stress, fails to provide a proper description of material behavior in this situation, so that more sophisticated flow theories are required. This point is made strongly by Sewell,[11] who shows that bifurcation buckling is quite sensitive to the direction of the normal to the loading surface and that, consequently, the shape of this surface in a local region near the stress point is very important.

Batdorf[12] discusses this point and shows, on a qualitative basis, that the slip theory of Batdorf and Budiansky can provide an explanation of plastic buckling behavior. He also states that the qualitative argument presented "justifies the use of deformation theory in the analysis of the plastic buckling of plates."

The other explanation is that the plastic buckling of plates and shells is sensitive to small imperfections, so that the treatment of the problem as a bifurcation phenomenon may lead to errors. This has been shown by Onat and Drucker[13] in an analysis of the torsional buckling of a compressively loaded member of hollow cruciform cross section. Besseling[14] extended this work to the case of a member of solid cruciform cross section and reached similar conclusions.

Although these theoretical objections to bifurcation buckling analysis based on deformation theory do exist, agreement with experiment suggests the use of such analysis in engineering computations (Ref. 15). Consequently, a plastic buckling theory based on a deformation theory of plasticity was used in the present analysis. The manner of introducing deformation theory is based on the work of Stowell.[8]

Although the Stowell theory is used, it should be noted that the basic procedure developed in the present work can readily accommodate other plasticity theories. All that is necessary to incorporate another theory is to redefine certain coefficients that enter into the modified bending stiffness matrix.

## Development of the Basic Procedure

The technique presented here is based on the displacement method of finite-element analysis. In this method, the matrix equation relating generalized nodal forces to generalized nodal displacements is

$$\{f\} = [K]\{\delta\} \tag{1}$$

where $\{f\}$ is the vector of generalized nodal forces in the

Received October 28, 1968; revision received February 26, 1969. This research was supported by the NASA Langley Research Center under Contract NAS 1-5040.

* Research Engineer.
† Head, Applied Mechanics Group. Associate Fellow AIAA.

transverse direction, $[K]$ is the total stiffness matrix of the structure, and $\{\delta\}$ is the vector of generalized nodal displacements in the transverse direction.

As discussed previously, the stiffness matrix can be separated into two parts: $[K] = [K_B] + [K_M]$. The bending stiffness matrix $[K_B]$ is a function of the plate material properties. When modified to include the effect of plasticity, it is a function of the current state of plastic deformation, and is, therefore, a nonlinear function of stress. The initial stress stiffness matrix $[K_M]$ is based on geometric considerations, as well as being a linear function of the stress state immediately prior to buckling.

The buckling problem is formulated on the basis of the homogeneous problem associated with Eq. (1),

$$[K]\{\delta\} = ([K_B] + [K_M])\{\delta\} = 0 \tag{2}$$

Equation (2) is satisfied for a nonzero displacement vector only if the stiffness matrix is singular. Therefore, the critical stress is reached when the stiffness matrix becomes singular, and the buckling criterion can be represented by the vanishing of the determinant of the stiffness matrix, $\det([K_B] + [K_M]) = 0$. This criterion is equivalent to the statement that the critical stress state causes the second variation of potential energy to be positive semidefinite (Ref. 16).

Computation of critical stresses can be most efficiently accomplished by recasting Eq. (2) into the form of an eigenvalue problem. To this end, a parameter $\lambda$ is introduced into Eq. (2),

$$([K_B] + \lambda[K_M])\{\delta\} = 0 \tag{3}$$

This parameter assumes values such that $\det([K_B] + \lambda[K_M])$ is equal to zero for the stress state used in the computation of the matrices $[K_B]$ and $[K_M]$. If this stress state is the critical one, $\lambda$ will be equal to one. Therefore, we have converted the buckling criterion to the requirement that $\lambda = 1$. Equation (3) then assumes the form of an eigenvalue equation,

$$-[K_M]\{\delta\} = (1/\lambda)[K_B]\{\delta\} \tag{4a}$$

or

$$[K_B]\{\delta\} = -\lambda[K_M]\{\delta\} \tag{4b}$$

The procedure for determining the buckling load is as follows. At some trial loading level, the stress state is calculated, and the matrices $[K_M]$ and $[K_B]$ are computed based on these stresses. The eigenvalue equation [Eq. (4)] is then solved and the lowest value of $\lambda$ examined. If this value is equal to one, the stated buckling criterion is satisfied and the trial loading is the critical one, i.e., $\det([K_B] + [K_M]) = 0$. If $\lambda$ is greater (less) than one, the trial loading level is less (greater) than the desired critical state. In this case the load is incremented (decremented) and the procedure is repeated. Thus, a succession of eigenvalue problems must be solved for various stress levels in order to establish the critical buckling load.

The formulation of the buckling problem in terms of the eigenvalue equation [Eq. (4)] has some basic advantages. It eliminates the possibility of missing the fundamental buckling mode, a possibility which exists when the determinant criterion is used. Furthermore, buckling mode shapes can be readily obtained. A discussion of the algorithms used in the present work for the solution of the eigenvalue problem can be found in Refs. 17 and 18.

## Application of the Stowell-Ilyushin Theory of Plastic Buckling

Ilyushin[7] presents a plastic buckling theory based on a deformation theory of plasticity. His formulation includes the possibility of elastic unloading, during buckling, in a portion of a cross section that is completely plastic in the prebuckling state.

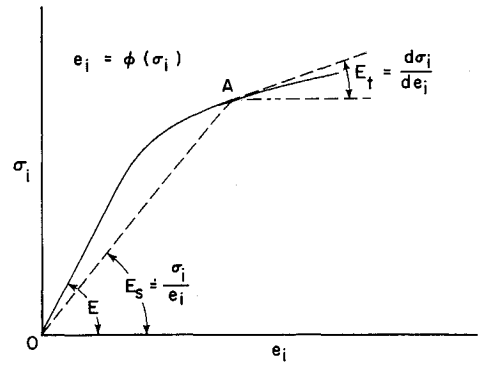


**Fig. 1 Typical effective stress-strain curve.**

Stowell[8] simplifies the analysis of Ref. 7 on the basis of results for the plastic buckling of columns. He assumes that, during buckling, there is no further change in the membrane stresses, and that a completely plastic cross section remains completely plastic; that is, there is no elastic unloading. These assumptions, along with the further restriction to a constant stress field in the prebuckling configuration, significantly reduce the complexity of the analysis, since the possibility of an elastic-plastic boundary in the cross section of the buckled configuration is excluded.

Stowell's analysis makes use of the concept of effective stress and effective strain, defined respectively for plane stress, as

$$\sigma_i = (\sigma_x^2 + \sigma_y^2 - \sigma_x\sigma_y + 3\tau_{xy}^2)^{1/2} \tag{5}$$

$$e_i = 2/(3)^{1/2}(e_x^2 + e_y^2 + e_xe_y + \gamma_{xy}^2/4)^{1/2} \tag{6}$$

where $e_x$, $e_y$, and $\gamma_{xy}$ are total strains. These quantities are assumed to be uniquely related as follows:

$$e_i = \varphi(\sigma_i) = \sigma_i/E_s \tag{7}$$

where $E_s$ is a secant modulus defined by this relation.

The stress-strain relations which are consistent with Eq.(7) are

$$e_x = \frac{1}{E_s}(\sigma_x - \tfrac{1}{2}\sigma_y),\ e_y = \frac{1}{E_s}(\sigma_y - \tfrac{1}{2}\sigma_x),\ \gamma_{xy} = \frac{3\tau_{xy}}{E_s}$$

Figure 1 shows a typical curve of effective stress vs effective strain. Such curves are based on uniaxial stress-strain characteristics determined experimentally. Also shown are the secant modulus $E_s = \sigma_i/e_i$ and the tangent modulus $E_t = d\sigma_i/de_i$. Throughout the present analysis, the functional relation between effective strain and effective stress is approximated by the Ramberg-Osgood[19] stress-strain relation.

The foregoing assumptions are used, along with the usual assumptions of classical plate theory,[20] to develop the pertinent moment-curvature relations for a slightly out-of-plane deformed configuration. The resulting relations explicitly contain the effect of plastic yielding prior to buckling.

The moment-curvature relations from Ref. 8 are

$$\begin{Bmatrix} M_x \\ M_y \\ 2M_{xy} \end{Bmatrix} = -D' \begin{bmatrix} C_1 & \tilde{C}_3 & -\frac{C_2}{2} \\ \tilde{C}_3 & C_5 & -\frac{C_4}{2} \\ -\frac{C_2}{2} & -\frac{C_4}{2} & 2\tilde{C}_3 \end{bmatrix} \begin{Bmatrix} \chi_1 \\ \chi_2 \\ \chi_3 \end{Bmatrix} \tag{8}$$

where

$$\chi_1 = \frac{\partial^2 w}{\partial x^2},\quad \chi_2 = \frac{\partial^2 w}{\partial y^2},\quad \chi_3 = \frac{\partial^2 w}{\partial x \partial y}$$

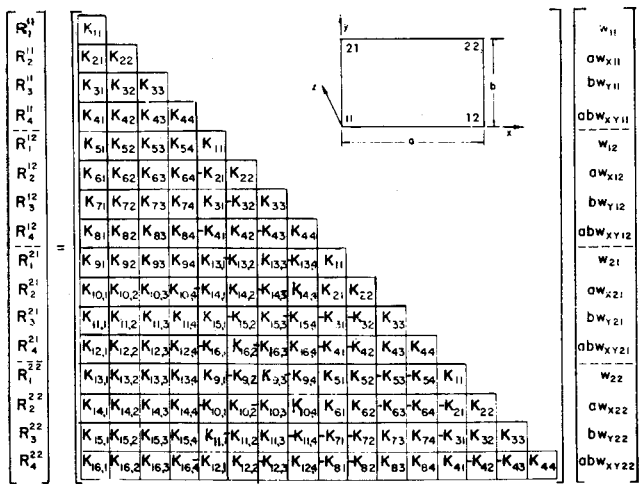

**Fig. 2a Arrangement of the stiffness matrices (pattern used with component parts multiplied by $C_1$, $C_5$, $\bar{C}_3$, $\bar{C}_3$, $\sigma_x$, $\sigma_y$).**

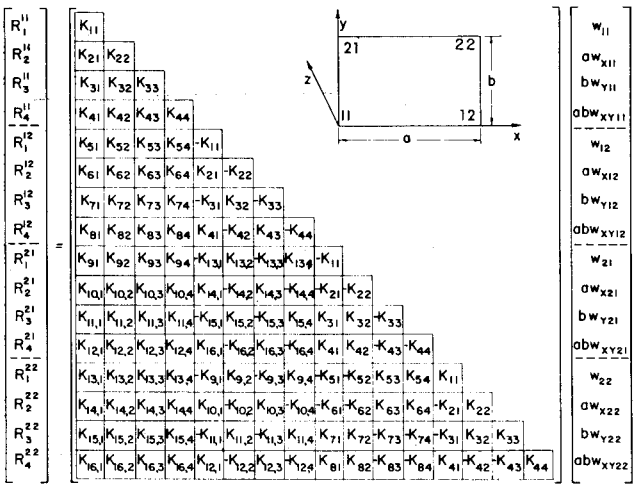

**Fig. 2b Arrangement of the stiffness matrices (pattern used with component parts multiplied by $C_2$, $C_4$, $\tau_{xy}$).**

are the curvature and twist in terms of the transverse deflection,

$$\begin{Bmatrix} M_x \\ M_y \\ M_{xy} \end{Bmatrix} = \int_{-h/2}^{h/2} z \begin{Bmatrix} \sigma_x \\ \sigma_y \\ \tau_{xy} \end{Bmatrix} dz$$

defines the bending and twisting moments, $h$ is the plate thickness, and $D' = E_s h^3/9$;

$$C_1 = 1 - \frac{3}{4}\frac{\sigma_x^2}{\sigma_i^2}\left(1 - \frac{E_t}{E_s}\right), \quad C_2 = 3\frac{\sigma_x \tau_{xy}}{\sigma_i^2}\left(1 - \frac{E_t}{E_s}\right)$$

$$\bar{C}_3 = \frac{1}{2}\left[1 - \frac{3}{2}\frac{\sigma_x \sigma_y}{\sigma_i^2}\left(1 - \frac{E_t}{E_s}\right)\right]$$

$$\bar{C}_3 = \frac{1}{2}\left[1 - 3\frac{\tau_{xy}^2}{\sigma_i^2}\left(1 - \frac{E_t}{E_s}\right)\right] \qquad (9)$$

$$C_4 = 3\frac{\sigma_y \tau_{xy}}{\sigma_i^2}\left(1 - \frac{E_t}{E_s}\right), \quad C_5 = 1 - \frac{3}{4}\frac{\sigma_y^2}{\sigma_i^2}\left(1 - \frac{E_t}{E_s}\right)$$

In order to formulate the plastic buckling problem for a finite-element analysis, it is necessary to develop the strain energy functional based on the moment-curvature relation of Eq. (8). Towards this end, we employ the following expression for the strain energy of bending in terms of moments and curvatures:

$$U_B = -\frac{1}{2}\int_A [M_x\chi_1 + M_y\chi_2 + 2M_{xy}\chi_3]dxdy \qquad (10)$$

Substituting the moment-curvature relation Eq. (8) into Eq. (10), we obtain the functional

$$U_B = \frac{D'}{2}\int_A (C_1\chi_1^2 - C_2\chi_1\chi_3 + 2[\bar{C}_3\chi_1\chi_2 + \bar{C}_3\chi_3^2] - C_4\chi_2\chi_3 + C_5\chi_2^2)dxdy \qquad (11)$$

When the contribution from the membrane stress field (Ref. 20, p. 387) is added to Eq. (11), we obtain the complete energy functional shown in matrix form as

$$U = \frac{1}{2}\int_A D' \begin{Bmatrix} \chi_1 \\ \chi_2 \\ \chi_3 \end{Bmatrix}^{\mathrm{T}} \begin{bmatrix} C_1 & \bar{C}_3 & -\frac{C_2}{2} \\ \bar{C}_3 & C_5 & -\frac{C_4}{2} \\ -\frac{C_2}{2} & -\frac{C_4}{2} & 2\bar{C}_3 \end{bmatrix} \begin{Bmatrix} \chi_1 \\ \chi_2 \\ \chi_3 \end{Bmatrix} dxdy + \frac{h}{2}\int_A \begin{Bmatrix} \frac{\partial w}{\partial x} \\ \frac{\partial w}{\partial y} \end{Bmatrix}^{\mathrm{T}} \begin{bmatrix} \sigma_x^0 & \tau_{xy}^0 \\ \tau_{xy}^0 & \sigma_y^0 \end{bmatrix} \begin{Bmatrix} \frac{\partial w}{\partial x} \\ \frac{\partial w}{\partial y} \end{Bmatrix} dxdy \qquad (12)$$

where $\sigma_x^0$, $\sigma_y^0$, $\tau_{xy}^0$ are the membrane stresses prior to buckling. This expression is identical in form with the expression for the strain energy of an anisotropic plate.[21]‡ The plate, therefore, deforms as if it were anisotropic, the anisotropy being due to plastic deformation and, consequently, is a function of the state of stress in the prebuckling configuration. All available plastic buckling theories exhibit this behavior, so that in each of them an energy functional similar to Eq. (11) can be developed, differing from Eq. (11) only in the definition of the quantities $C_1$ through $C_5$.

## Development of the Element Stiffness Matrices

The techniques used in the development of the element stiffness matrices, and the application of these matrices in a finite-element elastic analysis, have been discussed previously by a number of authors. The derivation of the initial-stress stiffness matrix in the present work follows specifically from the analysis presented in Ref. 4. That is, the energy functional associated with the deformation of a finite element is written in terms of the nodal generalized displacements. The element stiffness matrices are then derived from Castigliano's first theorem, where

$$k_{ij} = \partial^2 U/\partial\delta_i\partial\delta_j \qquad (13)$$

where $k_{ij}$ is an element in the stiffness matrix, $\delta_i,\delta_j$ are generalized nodal displacements, and $U$ is the energy functional associated with the element deformation. Once developed, the element stiffness matrices can be formed into the over-all stiffness matrix of the complete idealized structure by applying compatibility and equilibrium conditions at each node.

For the case of plastic buckling, Eq. (13) is used in conjunction with Eq. (12), the first integral yielding the bending stiffness matrix with the inclusion of the effect of plasticity, whereas the second integral yields the initial stress stiffness matrix.

Attention is restricted in the present treatment of plastic buckling to flat rectangular panels idealized by a network of

‡ Equation (12) is in the form of the energy functional for an anisotropic elastic plate when the following substitutions are made: $D'C_1 = D_{11}$; $D'C_2 = -4D_{16}$; $D'\bar{C}_3 = D_{12}$; $D'\bar{C}_3 = 2D_{66}$; $D'C_4 = -4D_{26}$; $D'C_5 = D_{22}$, where $D_{ij}$ describes the material properties of the plate as defined in Ref. 21.

$K_{mx} =$

| | | | |
|---|---|---|---|
| 1872 | 156 | 264 | 22 |
| 156 | 208 | 22 | 88/3 |
| 264 | 22 | 48 | 4 |
| 22 | 88/3 | 4 | 16/3 |
| -1872 | -156 | -264 | -22 |
| 156 | -52 | 22 | -22/3 |
| -264 | -22 | -48 | -4 |
| 22 | -22/3 | 4 | -4/3 |
| 648 | 54 | 156 | 13 |
| 54 | 72 | 13 | 52/3 |
| -156 | -13 | -36 | -3 |
| -13 | -52/3 | -3 | -4 |
| -648 | -54 | -156 | -13 |
| 54 | -18 | 13 | -13/3 |
| 156 | 13 | 36 | 3 |
| -13 | 13/3 | -3 | 1 |

$K_{my} =$

| | | | |
|---|---|---|---|
| 1872 | 264 | 156 | 22 |
| 264 | 48 | 22 | 4 |
| 156 | 22 | 208 | 88/3 |
| 22 | 4 | 88/3 | 16/3 |
| 648 | 156 | 54 | 13 |
| -156 | -36 | -13 | -3 |
| 54 | 13 | 72 | 52/3 |
| -13 | -3 | -52/3 | -4 |
| -1872 | -264 | -156 | -22 |
| -264 | -48 | -22 | -4 |
| 156 | 22 | -52 | -22/3 |
| 22 | 4 | -22/3 | -4/3 |
| -648 | -156 | -54 | -13 |
| 156 | 36 | 13 | 3 |
| 54 | 13 | -18 | -13/3 |
| -13 | -3 | 13/3 | 1 |

$K_{mxy} =$

| | | | |
|---|---|---|---|
| 150 | 0 | 0 | -6 |
| 0 | 0 | 6 | 0 |
| 0 | 6 | 0 | 0 |
| -6 | 0 | 0 | 0 |
| 0 | 0 | 30 | 6 |
| 0 | 0 | -6 | -1 |
| -30 | -6 | 0 | 0 |
| 6 | 1 | 0 | 0 |
| 0 | 30 | 0 | 6 |
| -30 | 0 | -6 | 0 |
| 0 | -6 | 0 | -1 |
| 6 | 0 | 1 | 0 |
| -150 | -30 | -30 | -6 |
| 30 | 5 | 6 | 1 |
| 30 | 6 | 5 | 1 |
| -6 | -1 | -1 | -1/6 |

**Fig. 3a First four columns of the component parts of the initial stress stiffness matrix.**

$K_{\bar{C}_3} =$

| | | | |
|---|---|---|---|
| 36 | 18 | 18 | 11/4 |
| 18 | 4 | 61/4 | 2 |
| 18 | 61/4 | 4 | 2 |
| 11/4 | 2 | 2 | 4/9 |
| -36 | -3 | -18 | -1.5 |
| 3 | -1 | -1.5 | -.5 |
| -18 | 1.5 | -4 | -1/3 |
| 1.5 | -.5 | 1/3 | -1/9 |
| -36 | -18 | -3 | -1.5 |
| -18 | -4 | -1.5 | -1/3 |
| 3 | 1.5 | -1 | -.5 |
| 1.5 | 1/3 | -.5 | -1/9 |
| 36 | 3 | 3 | .25 |
| -3 | 1 | -.25 | 1/12 |
| -3 | -.25 | 1 | 1/12 |
| .25 | -1/12 | -1/12 | 1/36 |

$K_{C_2} =$

| | | | |
|---|---|---|---|
| 0 | 0 | 0 | .1 |
| 0 | -.25 | -.1 | 0 |
| 0 | -.1 | 0 | 0 |
| .1 | 0 | 0 | 0 |
| 0 | 0 | 0 | -.1 |
| 0 | 0 | .1 | .05 |
| 0 | .1 | 0 | 0 |
| -.1 | -.05 | 0 | 0 |
| 0 | -.5 | 0 | -.1 |
| .5 | 0 | .1 | 0 |
| 0 | .1 | 0 | 1/60 |
| -.1 | 0 | -1/60 | 0 |
| 0 | .5 | 0 | .1 |
| -.5 | -.25 | -.1 | -.05 |
| 0 | -.1 | 0 | -1/60 |
| .1 | .05 | 1/60 | 1/120 |

$K_{C_4} =$

| | | | |
|---|---|---|---|
| 0 | 0 | 0 | .1 |
| 0 | 0 | -.1 | 0 |
| 0 | -.1 | -.25 | 0 |
| .1 | 0 | 0 | 0 |
| 0 | 0 | -.5 | -.1 |
| 0 | 0 | .1 | 1/60 |
| .5 | .1 | 0 | 0 |
| -.1 | -1/60 | 0 | 0 |
| 0 | 0 | 0 | -.1 |
| 0 | 0 | .1 | 0 |
| 0 | .1 | 0 | .05 |
| -.1 | 0 | -.05 | 0 |
| 0 | 0 | .5 | .1 |
| 0 | 0 | -.1 | -1/60 |
| -.5 | -.1 | -.25 | -.05 |
| .1 | 1/60 | .05 | 1/120 |

**Fig. 3b First four columns of the bending stiffness matrix (component parts multiplied by $\bar{C}_3$, $C_2$, $C_4$).**

$K_{C_1} =$

| | | | |
|---|---|---|---|
| 156 | 78 | 22 | 11 |
| 78 | 52 | 11 | 22/3 |
| 22 | 11 | 4 | 2 |
| 11 | 22/3 | 2 | 4/3 |
| -156 | -78 | -22 | -11 |
| 78 | 26 | 11 | 11/3 |
| -22 | -11 | -4 | -2 |
| 11 | 11/3 | 2 | 2/3 |
| 54 | 27 | 13 | 13/2 |
| 27 | 18 | 13/2 | 13/3 |
| -13 | -13/2 | -3 | -3/2 |
| -13/2 | -13/3 | -3/2 | -1 |
| -54 | -27 | -13 | -13/2 |
| 27 | 9 | 13/2 | 13/6 |
| 13 | 13/2 | 3 | 3/2 |
| -13/2 | -13/6 | -3/2 | -1/2 |

$K_{C_5} =$

| | | | |
|---|---|---|---|
| 156 | 22 | 78 | 11 |
| 22 | 4 | 11 | 2 |
| 78 | 11 | 52 | 22/3 |
| 11 | 2 | 22/3 | 4/3 |
| 54 | 13 | 27 | 13/2 |
| -13 | -3 | -13/2 | -3/2 |
| 27 | 13/2 | 18 | 13/3 |
| -13/2 | -3/2 | -13/3 | -1 |
| -156 | -22 | -78 | -11 |
| -22 | -4 | -11 | -2 |
| 78 | 11 | 26 | 11/3 |
| 11 | 2 | 11/3 | 2/3 |
| -54 | -13 | -27 | -13/2 |
| 13 | 3 | 13/2 | 3/2 |
| 27 | 13/2 | 9 | 13/6 |
| -13/2 | -3/2 | -13/6 | -1/2 |

$K_{\tilde{C}_3} =$

| | | | |
|---|---|---|---|
| 36 | 3 | 3 | .25 |
| 3 | 4 | .25 | 1/3 |
| 3 | .25 | 4 | 1/3 |
| .25 | 1/3 | 1/3 | 4/9 |
| -36 | -3 | -3 | -.25 |
| 3 | -1 | .25 | -1/12 |
| -3 | -.25 | -4 | -1/3 |
| .25 | -1/12 | 1/3 | -1/9 |
| -36 | -3 | -3 | -.25 |
| -3 | -4 | -.25 | -1/3 |
| 3 | .25 | -1 | -1/12 |
| .25 | 1/3 | -1/12 | -1/9 |
| 36 | 3 | 3 | .25 |
| -3 | 1 | -.25 | 1/12 |
| -3 | -.25 | 1 | 1/12 |
| .25 | -1/12 | -1/12 | 1/36 |

**Fig. 3c First four columns of the bending stiffness matrix (component parts multiplied by $C_1$, $C_5$, $\tilde{C}_3$).**

flat rectangular finite elements. The determination of the stiffness matrix for the individual elements is based on the use of a displacement function in the form of Hermitian polynomials, as proposed by Bogner, Fox, and Schmit.[22] This displacement function provides for compatibility of rotations and deflections between elements along their interfaces. It yields an element stiffness matrix of order $16 \times 16$. The results presented in Ref. 22 for elastic plate bending using this formulation indicate rapid monotonic convergence to the correct solution when the idealization is successively

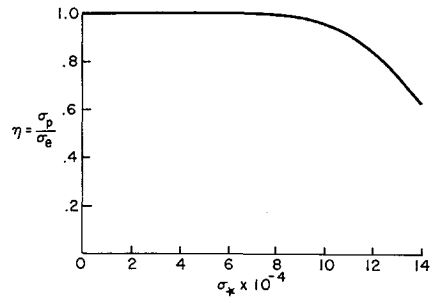


**Fig. 4 Plasticity reduction factor for a clamped square plate with a uniform compressive load on two opposite edges.**

refined. A series of calculations were performed in Ref. 23 for the purpose of evaluating the element stiffness matrix of Bogner, Fox, and Schmit for elastic buckling calculations. These results indicate rapid convergence to exact solutions when the idealization is successively refined.

Introduction of the assumed displacement function of Ref. 22 into Eqs. (12) and (13) yields the appropriate element stiffness matrices. These matrices can be written as

$$[K_B] = \frac{D'}{ab}\left[\frac{C_1}{35}\left(\frac{b}{a}\right)^2 [K_{C1}] + C_2\left(\frac{b}{a}\right)[K_{C2}] + \frac{1}{25}\bar{C}_3[K_{\bar{C}3}] + \frac{1}{25}\bar{C}_3[K_{\bar{C}3}] + C_4\left(\frac{a}{b}\right)[K_{C4}] + \frac{C_5}{35}\left(\frac{a}{b}\right)^2 [K_{C5}]\right] \quad (14)$$

$$[K_M] = \left[\frac{\sigma_x{}^0 h}{4200}\left(\frac{b}{a}\right)[K_{Mx}] + \frac{\sigma_y{}^0 h}{4200}\left(\frac{a}{b}\right)[K_{My}] + \frac{\tau_{xy}{}^0 h}{300}[K_{Mxy}]\right] \quad (15)$$

where $[K_{C1}]$, etc. and $[K_{Mx}]$, etc. are numerical matrices which are independent of the coefficients $C_1$–$C_5$ and the membrane stresses. Only the elements in the first four columns of these latter matrices need be computed, since values for these elements reappear in the remaining columns according to the pattern shown in Figs. 2a and 2b. Numerical values for the first four columns of these matrices are given in Figs. 3a, 3b, and 3c.

**Table 1 Plastic buckling of a simply supported square plate with various normal edge loadings; $a$ = 20 in., $b$ = 20 in., $E = 10^7$ psi, $\nu = \frac{1}{2}$, $\sigma_{0.7} = 10^5$ psi, $n$ = 10**

| Thickness $h$, in. | $\sigma_*$ exact | $\sigma_*$, finite-element analysis |
|---|---|---|
| | $\alpha = 1, \beta = 0, \gamma = 0$ | |
| 0.77867 | −65,000 | −65,002 |
| 0.85800 | −75,000 | −75,003 |
| 0.96449 | −85,000 | −85,003 |
| 1.12019 | −95,000 | −95,002 |
| 1.36678 | −105,000 | −105,002 |
| 1.76752 | −115,000 | −115,000 |
| 2.39053 | −125,000 | −125,002 |
| | $\alpha = 1.0, \beta = 1.0, \gamma = 0$ | |
| 1.12500 | −65,000 | −65,018 |
| 1.29980 | −75,000 | −75,014 |
| 1.60231 | −85,000 | −85,009 |
| 2.08258 | −95,000 | −95,008 |
| 2.77755 | −105,000 | −105,007 |
| 3.78569 | −115,000 | −115,007 |
| 5.26002 | −125,000 | −125,007 |
| | $\alpha = 1.0, \beta = 0.5, \gamma = 0$ | |
| 0.94979 | −65,000 | −65,020 |
| 1.03884 | −75,000 | −75,016 |
| 1.15727 | −85,000 | −85,015 |
| 1.33364 | −95,000 | −95,010 |
| 1.58816 | −105,000 | −105,008 |
| 1.93707 | −115,000 | −115,007 |
| 2.42382 | −125,000 | −125,007 |

## Discussion of Results

In order to evaluate the method of analysis developed, a number of calculations have been performed on the buckling of flat rectangular plates with various boundary and loading conditions. Results of a series of plastic buckling calculations for simply supported plates with various uniform edge loadings are presented and compared with exact results. Results are then shown for plastic buckling in cases for which exact solutions are lacking. These are: 1) a clamped square plate with a uniform load on two opposite edges, 2) a simply supported square plate with a triangular load distribution on two opposite edges, and 3) a simply supported plate with a uniform edge shear load.

In all of the plastic buckling calculations, the secant and tangent moduli were found using the Ramberg-Osgood stress-strain representation,

$$e_i = \sigma_i/E + (3\sigma_i/7E)[\sigma_i/\sigma_{0.7}]^{(n-1)} \quad (16)$$

where $n$ is a shape parameter given by

$$n = 1 + \log(\tfrac{1}{7})/\log(\sigma_{0.7}/\sigma_{0.85}) \quad (17)$$

and $e_i$ is effective strain, $E$ is the slope of the linear portion of the stress-strain curve, and $\sigma_{0.7}$ and $\sigma_{0.85}$ are the stresses at which the curve has secant moduli of $0.7E$ and $0.85E$, respectively. The tangent and secant moduli expressed as ratios of the elastic modulus are then given, respectively, by

$$\frac{E_t}{E} = \frac{1}{1 + (3n/7)(\sigma_i/\sigma_{0.7})^{n-1}} \quad (18)$$

**Table 2 Plastic buckling of a simply supported rectangular plate with various normal edge loadings; $a$ = 30 in., $b$ = 20 in., $E = 10^7$ psi, $\nu = \frac{1}{2}$, $\sigma_{0.7} = 10^5$ psi, $n$ = 10**

| Thickness $h$, in. | $\sigma_*$ exact | $\sigma_*$, finite-element analysis |
|---|---|---|
| | $\alpha = 1, \beta = 0, \gamma = 0$ | |
| 0.75088 | −65,000 | −65,005 |
| 0.83518 | −75,000 | −75,004 |
| 0.95429 | −85,000 | −85,004 |
| 1.12710 | −95,000 | −95,002 |
| 1.39064 | −105,000 | −105,001 |
| 1.80884 | −115,000 | −115,001 |
| 2.45321 | −125,000 | −125,001 |
| | $\alpha = 1.0, \beta = 1.0, \gamma = 0$ | |
| 0.95460 | −65,000 | −65,025 |
| 1.10292 | −75,000 | −75,016 |
| 1.35960 | −85,000 | −85,011 |
| 1.76713 | −95,000 | −95,010 |
| 2.35683 | −105,000 | −105,009 |
| 3.21226 | −115,000 | −115,009 |
| 4.46327 | −125,000 | −125,009 |
| | $\alpha = 1.0, \beta = 0.5, \gamma = 0$ | |
| 0.84370 | −65,000 | −65,022 |
| 0.92558 | −75,000 | −75,018 |
| 1.03918 | −85,000 | −85,015 |
| 1.21632 | −95,000 | −95,009 |
| 1.48109 | −105,000 | −105,008 |
| 1.84729 | −115,000 | −115,007 |
| 2.35015 | −125,000 | −125,007 |

**Table 3 Plastic buckling of a clamped square plate with a uniform load on two opposite edges; $a = 20$ in., $b = 20$ in., $\nu = \frac{1}{2}$, $E = 10^7$ psi, $\sigma_{0.7} = 10^5$ psi, $n = 10$, $\alpha = 1$, $\beta = 0$, $\gamma = 0$**

| Thickness $h$, in. | Critical stress, psi | Elastic critical stress, psi |
|---|---|---|
| 0.5 | −66,414 | −69,018 |
| 0.6 | −81,712 | −99,385 |
| 0.7 | −91,234 | −135,277 |
| 0.8 | −97,549 | −176,687 |

$$\frac{E_s}{E} = \frac{1}{1 + (\frac{3}{7})(\sigma_i/\sigma_{0.7})^{n-1}} \tag{19}$$

Values of $\sigma_{0.7} = 10^5$ psi and $n = 10$ were used in all the calculations. Since the Ramberg-Osgood relation does not identify a distinct yield point, all the calculations contain some effect of plasticity.

In order to determine the accuracy of the finite-element analysis when applied to the plastic buckling problem, a series of computations were performed and the results compared with corresponding exact solutions to the governing equations presented by Stowell in Ref. 8. The cases selected for comparison have simply supported edge conditions and uniformly distributed loads normal to the boundary. The procedure followed in these cases was to calculate a value of plate thickness, from Stowell's governing differential equation, corresponding to plastic buckling at a given membrane stress in the plastic range. Using this thickness, a value for the critical stress was then found by means of the finite-element procedure and compared with the initially assumed value.

Using this procedure, critical stresses were found for simply supported plates with length to width ratio $a/b = 1$ and $a/b = 1.5$ for three different loading situations: 1) $\sigma_x = -\sigma_*$, $\sigma_y = 0$; 2) $\sigma_x = \sigma_y = -\sigma_*$; and 3) $\sigma_x = 2\sigma_y = -\sigma_*$. The idealization used in these calculations consisted of square elements in a $4 \times 4$ grid when $a/b = 1$, and a $6 \times 4$ grid when $a/b = 1.5$. Symmetry was taken into account, so that it was necessary to consider only one-quarter of the plate.

Calculations were carried out for all three loading situations for a range of nominal stress ($\sigma_*$) of 65,000 to 125,000 psi. The results are shown in Tables 1 and 2. These results encompass a widely varying degree of plastic deformation at the critical stress. The tables show the thickness, the corresponding exact value of the nominal stress, and the stress computed from the finite-element analysis. The various loading situations are identified by the parameters

$$\alpha = -\frac{\sigma_x}{\sigma_*}, \quad \beta = -\frac{\sigma_y}{\sigma_*}, \text{ and } \gamma = -\frac{\tau_{xy}}{\sigma_*}$$

**Table 4 Plastic buckling of a simply supported square plate with a triangular edge load; $a = b = 20$ in., $\nu = 0.5$, $E = 10^7$ psi, $\sigma_{0.7} = 10^5$ psi, $n = 10$**

a) Plastic buckling stress distribution in the $y$ direction

| | Thickness $h$, in. | | | | |
|---|---|---|---|---|---|
| $y/b$ | 0.5 | 0.6 | 0.7 | 0.8 | 1.0 |
| 0 to 0.125 | −50,140 | −71,856 | −93,895 | −110,553 | −130,077 |
| 0.125 to 0.25 | −43,496 | −62,275 | −81,377 | −95,813 | −112,734 |
| 0.25 to 0.375 | −36,770 | −52,695 | −68,857 | −81,070 | −95,390 |
| 0.375 to 0.50 | −30,084 | −43,113 | −56,338 | −66,331 | −78,046 |
| 0.50 to 0.625 | −23,398 | −33,531 | −43,819 | −51,591 | −60,702 |
| 0.625 to 0.75 | −16,714 | −23,952 | −31,299 | −36,851 | −43,359 |
| 0.75 to 0.875 | −10,028 | −14,372 | −18,778 | −22,110 | −26,015 |
| 0.875 to 1.0 | −3,342 | −4,790 | −62,600 | −7,370 | −8,671 |

b) Normalized plastic buckling stress at $y = 0$

| Thickness $h$, in. | Critical stress, psi | Elastic critical stress, psi |
|---|---|---|
| 0.5 | −53,483 | −54,166 |
| 0.6 | −76,646 | −78,000 |
| 0.7 | −100,155 | −106,166 |
| 0.8 | −117,923 | −138,667 |
| 1.0 | −138,749 | −216,667 |

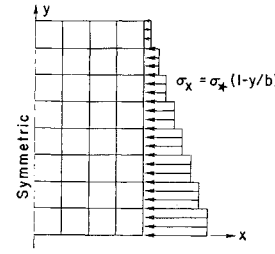


**Fig. 5 Idealization for simply supported square plate with a triangular compressive edge load.**

The results for the square plate (shown in Table 1) are based on a buckling mode shape consisting of a half-sine wave in each direction, and indicate agreement which is virtually exact. The maximum error was found to be +0.031%.

The results for the rectangular plate (shown in Table 2) are based on a buckling mode shape consisting of a full sine wave in the direction of the longer side and a half-sine wave in the direction of the shorter side. Agreement is again seen to be excellent, the maximum error in this case being +0.039%.

We now consider the case of a clamped square plate loaded uniformly on two opposite edges. Once more, taking into account the double symmetry of the buckling configuration, it is necessary to consider only one-quarter of the plate. The idealization that was used consisted of a $12 \times 12$ grid, and the error in the elastic case, using this idealization, was +0.058%. The plate considered has the dimensions $a = b = 20$ in.

Calculations were made for various thicknesses, ranging from $h = 0.5$ in. to $h = 0.8$ in. This thickness range corresponds to a range of buckling stress from a value close to the elastic limit up to a value well into the plastic range. Table 3 shows both plastic and elastic buckling stresses corresponding to the various thicknesses. As the state of stress penetrates further into the plastic range, the material stiffness decreases, so that the plastic buckling stress decreases relative to the corresponding elastic buckling stress. For $h = 0.8$ in., the maximum thickness considered, this decrease amounts to 44.8%. This can be seen graphically in Fig. 4, which shows the plasticity reduction factor $\eta$, defined as the ratio of the plastic buckling stress to the elastic buckling stress, $\sigma_P/\sigma_e$, plotted vs the plastic buckling stress.

The next case to be considered is that of a simply supported square plate with a triangular distribution of load on two opposite edges. It was selected to demonstrate the applicability of the method to nonconstant stress field situations. As mentioned previously, the Stowell formulation of the plastic buckling problem involves the assumption of a uniform stress state throughout the plate. This does not preclude the use of this formulation in a finite-element analysis of a plate that is not uniformly stressed. The stress can still be considered to be uniform within each element,

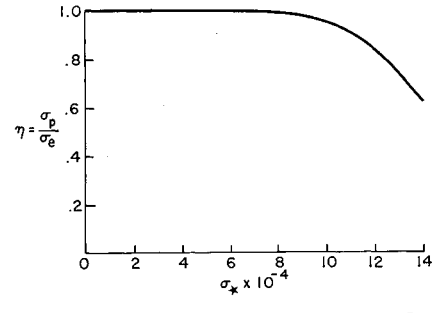


**Fig. 6 Plasticity reduction factor for a simply supported square plate with a triangular compressive load on two opposite edges.**

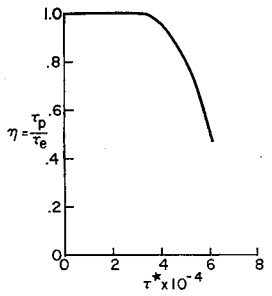


**Fig. 7 Plasticity reduction factor for a simply supported square plate with a uniform edge shear load.**

but can vary from element to element. The stress distribution is thus approximated in the form of finite jumps over the planform of the plate. The state of plasticity, consistent with the Stowell formulation, is therefore constant within each finite element. By taking advantage of the single symmetry of the buckling mode, only one-half of the plate need be considered. The idealization of the half-plate consists of 32 square elements, as shown in Fig. 5. The idealized stress distribution is also shown in Fig. 5.

To check the accuracy obtainable with such an idealization, an elastic case for a simply supported square plate, $a = b = 20$ in., was analyzed. The exact solution (taken from Ref. 24) can be written as

$$\sigma_* = kE\pi^2h^2/12(1 - \nu^2)b^2 \qquad (20)$$

where $\sigma_*$ is the stress intensity at $y = 0$, and $k$ is the elastic buckling coefficient. For the case considered, Ref. 24 gives a value of 7.8 for $k$. The finite-element analysis yielded the value $k = 7.8068$, which represents an error of only $+0.087\%$.

Plastic buckling calculations were carried out using the same idealization for thicknesses ranging from $h = 0.5$ in. to $h = 1$ in. The results, in the form of the idealized critical stress distribution in the $y$ direction, are presented in Table 4a. Each case represents a different degree of plastic deformation. The case $h = 0.5$ in. can be considered to be fully elastic. As a consequence of not defining a definite yield point, however, there is still a small reduction of the buckling stress due to the inclusion of a small plasticity effect. A noticeable departure from linearity in the stress-strain relation occurs at about 70,000 psi. Therefore, on the basis of this value as the yield stress, we can trace an elastic-plastic boundary in the idealized structure. This boundary is indicated by a dashed line in Table 4a. As the thickness increases, the number of elements stressed beyond the yield point at the critical load also increases. When $h = 1$ in., half the plate is in the plastic range when the critical stress is reached.

In Table 4b, the normalized buckling stress (the maximum value in the triangular distribution) is shown for the various thicknesses, and compared with the corresponding elastic results. A plot of the plasticity reduction factor $\eta$ vs the plastic buckling stress is shown in Fig. 6.

The effectiveness of the assumed element displacement function when applied to the buckling analysis of a plate loaded in pure shear is considered next. The case of a simply supported square plate with an idealization consisting of a $6 \times 6$ grid of square elements was studied. Calculations to determine the elastic buckling coefficient, using this idealization, yielded the value, $k = 9.3458$, as compared to a value of 9.34 given by a series solution.[24]

The results of plastic buckling calculations are shown in Table 5. As before, the plastic buckling stress is compared with corresponding elastic buckling results for a range of thicknesses. The plasticity reduction factor $\eta$ is shown vs the plastic buckling stress in Fig. 7.

**Table 5 Plastic buckling of a simply supported square plate due to a uniform shear load; $a = 20$ in., $b = 20$ in., $\nu = 0.5$, $E = 10^7$ psi, $\sigma_{0.7} = 10^5$ psi, $n = 10$**

| Thickness $h$, in. | Critical stress, psi | Elastic critical stress, psi |
|---|---|---|
| 0.4 | −39,414 | −40,969 |
| 0.5 | −50,313 | −64,015 |
| 0.6 | −56,604 | −92,182 |
| 0 7 | −60,792 | −125,470 |

## Concluding Remarks

A finite-element method has been developed for the buckling analysis of flat rectangular plates stressed into the plastic range. Both simply supported and clamped edge conditions and arbitrary edge loadings can be taken into account. Computed results indicate that good accuracy may be obtained with a relatively coarse network of elements. The method can be readily applied to cases that would be difficult to analyze on a continuum basis.

## References

[1] Greene, B. C., "Stiffness Matrix for Bending of a Rectangular Plate Element with Initial Membrane Stresses," Structural Analysis Research Memo 45, Aug. 1962, The Boeing Co., Seattle, Wash.

[2] Kapur, K. K. and Hartz, B. J., "Stability of Plates Using the Finite Element Method," *Journal of Engineering Mechanics Division Proceedings of the American Society of Civil Engineers*, Vol. 92, No. EM 2, April 1966, p. 177.

[3] Gallagher, R. H. et al., "A Discrete Element Procedure for Thin-Shell Instability Analysis," *AIAA Journal*, Vol. 5, No. 1, Jan. 1967, pp. 138–145.

[4] Martin, H. C., "On the Derivation of Stiffness Matrices for the Analysis of Large Deflection and Stability Problems," *Proceedings of the Conference on Matrix Methods in Structural Mechanics*, Wright-Patterson Air Force Base, Dayton, Ohio, Oct. 1965; also AFFDL-TR-66-80, p. 697.

[5] Handelman, G. H. and Prager, W., "Plastic Buckling of a Rectangular Plate Under Edge Thrusts," Rept. 946, 1949, NACA.

[6] Pearson, C. E., "Bifurcation Criterion and Plastic Buckling of Plates and Columns," *Journal of the Aerospace Sciences*, Vol. 17, No. 7, July 1950, pp. 417–424.

[7] Ilyushin, A. A., "The Elasto-Plastic Stability of Plates," TM 1188, Dec. 1947, NACA.

[8] Stowell, E. Z., "A Unified Theory of Plastic Buckling of Columns and Plates," TR 898, 1948, NACA.

[9] Bijlaard, P. P., "Theory and Tests on the Plastics Stability of Plates and Shells," *Journal of the Aerospace Sciences*, Vol. 16, No. 9, Sept. 1949, pp. 529–541.

[10] Pride, R. A. and Heimerl, G. J., "Plastic Buckling of Simply Supported Compressed Plates," TN 1817, April 1949, NACA.

[11] Sewell, M. J., "A General Theory of Elastic and Inelastic Plate Failure—II," *Journal of Mechanics and Physics of Solids*, Vol. 12, Nov. 1964, p. 279.

[12] Batdorf, S. B., "Theories of Plastic Buckling," *Journal of the Aerospace Sciences*, Vol. 16, No. 7, July 1949, p. 405.

[13] Onat, E. T. and Drucker, D. C., "Inelastic Instability and Incremental Theories of Plasticity," *Journal of the Aerospace Sciences*, Vol. 20, No. 3, March 1953, p. 181.

[14] Besseling, J. F., "Analysis of the Plastic Collapse of a Cruciform Column with Initial Twist, Loaded in Compression," *Journal of the Aerospace Sciences*, Vol. 23, No. 1, Jan. 1956, p. 49.

[15] Gerard, G. and Becker, H., "Handbook of Structural Stability, Part I—Buckling of Flat Plates," TN 3781, July 1957, NACA.

[16] Langhaar, H. L., *Energy Methods in Applied Mechanics*, Wiley, New York, 1962, pp. 210–213.

[17] Armen, H., Jr. and Pifko, A., "Computer Programs for the Plastic Analysis of Structures Using Discrete Element Methods," NASA CR-66364, June 1967, Grumman Aircraft Engineering Corp., Bethpage, N. Y.

[18] Wilkinson, J. H., *The Algebraic Eigenvalue Problem*, Clarendon Press, Oxford, England, 1965, pp. 290–315.

[19] Ramberg, W. and Osgood, W. R., "Description of Stress-Strain Curves by Three Parameters," TN 902, 1943, NACA.

[20] Timoshenko, S. and Woinowsky-Krieger, S., *Theory of Plates and Shells*, McGraw-Hill, New York, 1959, p. 379.
[21] Lekhnitskii, S. G., "Anisotropic Plates," *Contributions to the Metallurgy of Steel*, No. 50, American Iron and Steel Institute, New York, 1956.
[22] Bogner, F. K., Fox, R. L., and Schmit, L. A., Jr., "The Generation of Interelement-Compatible Stiffness and Mass Matrices by the Use of Interpolation Formulas," *Proceedings of the Conference on Matrix Methods in Structural Mechanics*, Wright-Patterson Air Force Base, Dayton, Ohio, Oct. 1965; also AFFDL-TR-66-80, p. 397.
[23] Isakson, G., Armen, H., Jr., and Pifko, A., "Discrete-Element Methods for the Plastic Analysis of Structures," CR-803, Oct. 1967, NASA.
[24] Timoshenko, S. P. and Gere, J. M., *Theory of Elastic Stability*, McGraw-Hill, New York, 1961.

OCTOBER 1969 AIAA JOURNAL VOL. 7, NO. 10

# Static and Dynamic Applications of a High-Precision Triangular Plate Bending Element

G. R. Cowper,* E. Kosko,† G. M. Lindberg,* and M. D. Olson‡
*National Aeronautical Establishment, National Research Council of Canada, Ottawa, Canada*

**A fully conforming plate bending element of arbitrary triangular shape is developed and applied to the solution of several static and dynamic plate problems. The element incorporates 18 generalized coordinates, namely the transverse displacement and its first and second derivatives at each vertex. Example applications presented include static and dynamic analyses of a square plate with edges either simply supported or clamped, statics of an equilateral triangular simply supported plate, and vibrations of cantilevered triangular plates. Rates of convergence of the finite element approximations are investigated both theoretically and numerically. Excellent accuracy is achieved in all cases, and the rates of error convergence agree closely with predicted asymptotic values.**

## Nomenclature

| | | |
|---|---|---|
| $\{A\}$ | = | column vector of coefficients $a_i$, Eq. (7) |
| $a,b,c$ | = | element dimensions, Fig. 1 |
| $a_i$ | = | coefficients of quintic polynomial, Eq. (2) |
| $D$ | = | plate flexural rigidity = $Et^3/12(1-\nu^2)$ |
| $E$ | = | Young's modulus |
| $F(m,n)$ | = | modified Euler's beta function, Eq. (14) |
| $[K],[k]$ | = | stiffness matrices, Eqs. (12) and (18) |
| $L$ | = | length of side of square or triangular plate |
| $[M],[m]$ | = | consistent mass matrices, Eqs. (19) and (20) |
| $m_i,n_i$ | = | exponents of $\xi$, $\eta$ in $i$th term of polynomial, Eq. (2) |
| $N$ | = | number of elements per side of plate |
| $\{P\},\{p\}$ | = | consistent load vectors, Eqs. (22) and (23) |
| $[R],[T],$ $[T_1],[T_2]$ | = | transformation matrices, Sec. 2 |
| $t$ | = | thickness of plate |
| $\{W\},\{W_1\}$ | = | column vectors of generalized displacements, Eqs. (5) and (16) |
| $w$ | = | transverse displacement of plate |
| $w_x,w_{xy},\ldots$ | = | $\partial w/\partial x$, $\partial^2 w/\partial x\partial y\ldots$ |
| $x,y,\xi,\eta$ | = | global and local coordinates, respectively, Fig. 1 |
| $\theta$ | = | angle between global and local coordinates, Fig. 1 |
| $\lambda$ | = | eigenvalue = $\rho t\omega^2 L^4/D$ |
| $\nu$ | = | Poisson's ratio |
| $\rho$ | = | mass density of plate material |
| $\omega$ | = | circular frequency of plate vibration |

## 1.0 Introduction

THE finite element method has proved to be an extremely powerful tool for the analysis of discrete and continuous structures. A good introduction to the subject, which is undergoing rapid and continuing development, can be found in the books by Zienkiewicz[1] and Przemieniecki.[2]

A particularly useful area for the application of finite elements is the static and dynamic analysis of plate bending. Although many finite elements for plate bending have been developed in recent years, only elements of rectangular shape have so far met the requirements of high accuracy and good convergence. The most satisfactory of these is the sixteen degree-of-freedom rectangular element developed by Bogner, Fox, and Schmit,[3] Butlin and Leckie,[4] and later by Mason.[5] Rectangular elements are, however, unsuitable for a great variety of boundary shapes and there is a need for a general triangular element having adequate accuracy and convergence properties.

It is essential for convergence that a finite element be capable of representing a state of uniform strain; in the case of plate bending, this is a state of uniform curvature or uniform twist. Rigid body displacements, which are states of zero strain, should be included among the states of uniform strain. A further desirable property of a plate bending element is conformity. Conformity in this context means that slopes are continuous between elements, as well as transverse displacements. Several convergence proofs are now available for conforming elements, and such elements have the useful property of furnishing lower bounds on the actual strain energy of a plate. Under certain conditions this property can imply monotonic convergence of the strain energy.

Conforming triangular elements for plate bending have been developed by Bazeley et al.[6], and by Clough and Tocher,[7] but these allow only a linear variation of slope normal to an edge and give rather poor results. Suggested improvements to these elements require the introduction of additional nodes on the edges, but this has the inconvenience of making the programing more complicated.

In this paper, the authors present a general triangular element for plate bending that possesses the aforementioned desirable properties. It makes use of six deflection param-

Received January 30, 1969.
* Associate Research Officer, Structures and Materials Laboratory.
† Senior Research Officer.
‡ Assistant Research Officer. Member AIAA.